

# Preparation of transition metal composite graphite felt cathode for efficient heterogeneous electro-Fenton process

Liang Liang<sup>1,2</sup> · Fangke Yu<sup>1,2</sup> · Yiran An<sup>1,2</sup> · Mengmeng Liu<sup>1,2</sup> · Minghua Zhou<sup>1,2</sup>

Received: 29 January 2016 / Accepted: 4 August 2016 / Published online: 10 September 2016  
© Springer-Verlag Berlin Heidelberg 2016

**Abstract** A composite graphite felt (GF) modified with transition metal was fabricated and used as cathode in heterogeneous electro-Fenton (EF) for methyl orange (MO) degradation. Characterized by scanning electron microscopy (SEM) and X-ray photoelectron spectroscopy (XPS), the morphology and surface physicochemical properties of the cathodes after modification were observed considerably changed. After loading metals, the current response became higher, the accumulation of H<sub>2</sub>O<sub>2</sub> and the degradation efficiency of MO were improved. Under the same conditions, GF-Co had the highest catalytic activity for electro-reduction of O<sub>2</sub> to H<sub>2</sub>O<sub>2</sub> and MO degradation. At pH 3, 99 % of MO degradation efficiency was obtained using GF-Co after 120 min treatment and even at initial pH 9, 82 % of that was obtained. TOC removal efficiency reached 93.8 % using GF-Co at pH 3 after 120 min treatment while that was 12.3 % using GF. After ten-time runs, the mineralization ratio of the GF-Co was still 89.5 %, suggesting that GF-Co was very promising for wastewater treatment. The addition of isopropanol proved that ·OH played an important role in degradation of MO.

**Keywords** Heterogeneous electro-Fenton · Hydroxyl radical · Graphite felt · Transition metals · Methyl orange

Responsible editor: Philippe Garrigues

✉ Minghua Zhou  
zhoumh@nankai.edu.cn

<sup>1</sup> Key Laboratory of Pollution Process and Environmental Criteria, Ministry of Education, Tianjin, China

<sup>2</sup> Key Laboratory of Urban Ecology Environmental Remediation and Pollution Control, College of Environmental Science and Engineering, Nankai University, Tianjin 300350, China

## Introduction

Electro-Fenton (EF) is one of the powerful and widely used advanced oxidation processes (AOPs) for the treatment of industrial wastewater containing non-biodegradable organic pollutants (Brillas and Martinez-Huitle 2015; Martinez-Huitle et al. 2015; Sirés et al. 2014). The EF system can continuously supply H<sub>2</sub>O<sub>2</sub> through the two-electron reduction of oxygen on the cathode (Eq. 1). Meanwhile, Fe<sup>2+</sup> is added to react with H<sub>2</sub>O<sub>2</sub> for producing ·OH following Eq. (2) with the Fe<sup>2+</sup> regeneration by a direct cathodic reaction (Eq. 3) (Brillas et al. 2009).



However, the homogeneous EF requires an optimum of pH = 3 and a certain amounts of Fe<sup>2+</sup> and the effluent must be neutralized, which results in the generation of abundant sludge (Garcia-Segura et al. 2012; Wang et al. 2013b). So, heterogeneous EF oxidation has become prevalent for wastewater treatment, where soluble Fe<sup>2+</sup> is replaced by Fe containing solids without the need of low pH and iron sludge treatment (Ai et al. 2007b; Ammar et al. 2015; Dhakshinamoorthy et al. 2012; Feng et al. 2011; Navalon et al. 2011; Zhang et al. 2012).

In the past decades, the potential applications of heterogeneous catalysts have been investigated widely. Various kinds

of iron oxides and iron hydroxides, such as  $\text{Fe}_3\text{O}_4$ ,  $\alpha\text{-Fe}_2\text{O}_3$ , and  $\alpha\text{-FeOOH}$  have already been used to activate  $\text{H}_2\text{O}_2$ . However, many of them show lower catalytic activity than soluble  $\text{Fe}^{2+}$  and need the aid of ultrasound (Huang et al. 2012; Segura et al. 2012) and UV/visible light irradiation (Liang et al. 2012; Zhao et al. 2013), increasing the cost for wastewater treatment.

Recently, other ways have been developed to enhance the activity of heterogeneous catalysts, e.g., reducing the size of catalysts to nano-scale to increase the surface energy (Valdes-Solis et al. 2007), loading the catalysts on carriers with high surface area to improve their dispersion (Zhao et al. 2012). Many researchers also have developed new methods to obtain heterogeneous catalysts. For example, Wang et al. (2013a) used ferrite-carbon aerogel (FCA) monoliths with different iron/carbon ratios as heterogeneous catalyst for metalaxyl degradation. Wang et al. (2015b) used mesoporous copper ferrite (meso- $\text{CuFe}_2\text{O}_4$ ) as a heterogeneous EF catalyst for the degradation of organic contaminants.

In EF process, it is essential to choose an appropriate cathode material for effective production of  $\text{H}_2\text{O}_2$ . Carbonaceous materials are the most familiar materials used as cathode, such as graphite (Scialdone et al. 2013; Zhang et al. 2008a), carbon or graphite felt (Oturán et al. 2013; Panizza and Oturán 2011; Pimentel et al. 2008; Zhou et al. 2012), carbon sponge (Zcan et al. 2008, 2009), activated carbon fiber (Wang et al. 2005), and carbon-PTFE air-diffusion electrode (Brillas et al. 2000). Among them, graphite felt (GF) has been regarded as one of the most widely used cathode materials due to their large 3D active surface, mechanical integrity, commercial availability, easy acquisition, and efficient cathodic regeneration of  $\text{Fe}^{2+}$  (Zhou et al. 2012). To further improve the electro-catalytic activity of these carbonaceous materials, various attempts have been made for a more efficient  $\text{H}_2\text{O}_2$  production (Zhang et al. 2008b, c, 2009). Zhou et al. (2014) used ethanol and hydrazine hydrate to modify GF as cathode in EF system and showed the hydrogen peroxide accumulation increased by 160 % after modification. Bonakdarpour et al. (2011) reported metal-carbon composite catalysts for electro-synthesis of  $\text{H}_2\text{O}_2$  and showed Co-carbon had the best catalytic activity. In our previous work, a simple method using carbon black and PTFE was firstly developed to modify graphite felt and after modification, the yield of  $\text{H}_2\text{O}_2$  could be significantly increased by about 10.7 times (Yu et al. 2015a).

In the present work, we prepared metal-carbon graphite felt as cathode for EF process. The structure, morphology, and formation mechanism of the composite cathode were investigated. To evaluate its catalytic activity in the heterogeneous EF process, a model azo dye, methyl orange (MO), was chosen as the target pollutant.

## Experimental

### Transition metal-based catalysts and electrodes preparation

All chemicals used in this study were of analytical grade and used as received without further purification. The GF (Shanghai Qijie Carbon Material Co., Ltd.) were degreased in an ultrasonic bath with acetone and deionized water in sequence, dried at 80 °C for 24 h. Appropriate amounts of carbon black and metal nitrate salts were mixed in an ultrasonic bath for 30 min and dried overnight at 70 °C in an oven. The ferrous precursor consisted of  $\text{Fe}(\text{NO}_3)_2 \cdot 6\text{H}_2\text{O}$  with a 99.99 % purity. Similar nitrate salts were used for Co, Ce, and Cu as well. The mixture was heat treated in a ceramic tube furnace at 900 °C under flowing  $\text{N}_2$  for 2 h. The transition metal-based catalysts were marked as C-metal. Appropriate amounts of C-metal (0.3 g), PTFE, distilled water (30 mL), and *n*-butanol (3 %) were mixed in an ultrasonic bath for 10 min to create a highly dispersed mixture. The pretreated GF were immersed into the mixture and sonicated for 30 min and then dried at 80 °C for 24 h. At last, the samples were annealed at 360 °C for 30 min. The composite electrodes were marked as GF-C, GF-Fe, GF-Co, GF-Ce, and GF-Cu, respectively.

### Electro-generation of $\text{H}_2\text{O}_2$ and MO degradation

The  $\text{H}_2\text{O}_2$  electro-generation experiments were performed in an undivided cell (0.1 L) at the current density of 50  $\text{A}/\text{m}^2$  with 0.05 M  $\text{Na}_2\text{SO}_4$  as the supporting electrolyte at room temperature, stirring at 300 rpm with a magnetic bar. Ti/ $\text{IrO}_2$ - $\text{RuO}_2$  ( $4 \times 2$  cm) was used as anode and the modified GF ( $4 \times 5$  cm, thickness 5 mm) was selected as cathode. The distance between the anode and cathode was 2.5 cm. At time intervals, 1 mL samples were taken for analyzing the concentration of  $\text{H}_2\text{O}_2$ . The degradation of MO by EF process was carried out in the same apparatus at initial MO concentration of 50 mg/L at the current density of 50  $\text{A}/\text{m}^2$ . The solution pH was adjusted to 3 after 0.2 mM  $\text{Fe}^{2+}$  was added into the solution as the catalyst. The MO samples were taken to determine the degradation efficiency.

### Analysis

Linear sweep voltammetry (LSV) was carried out to compare the electro-chemical behavior during  $\text{H}_2\text{O}_2$  production. The performance was recorded by the CHI660D workstation (CH Instruments, Chenhua, Shanghai, China) at a scan rate of 10 mV/s in a three-electrode system (0.1 L), using the modified GF as the working electrode, Ti/ $\text{IrO}_2$ - $\text{RuO}_2$  as

counter electrode, and saturated calomel electrode (SCE) as the reference electrode at ambient temperature. The surface structure of the electrode was studied by scanning electron microscopy (SEM; LEO-1530VP, Germany). The surface elemental composition of the as-prepared electrodes were determined by XPS (Perkin-Elmer, a RBD upgraded PHI-5000 C ESCA system, Physical Electronics, USA) with Mg K radiation.

The concentration of  $H_2O_2$  was monitored by UV-Vis spectrophotometer (UV-2600, Shimadzu) at  $\lambda_{max} = 400$  nm using the potassium titanium (IV) oxalate method (Yu et al. 2015b). The current efficiency for  $H_2O_2$  production was calculated according to the formula (4) (Brillas et al. 2009):

$$CE (\%) = \frac{nFCV}{Q} \int_0^t I dt \times 100 \quad (4)$$

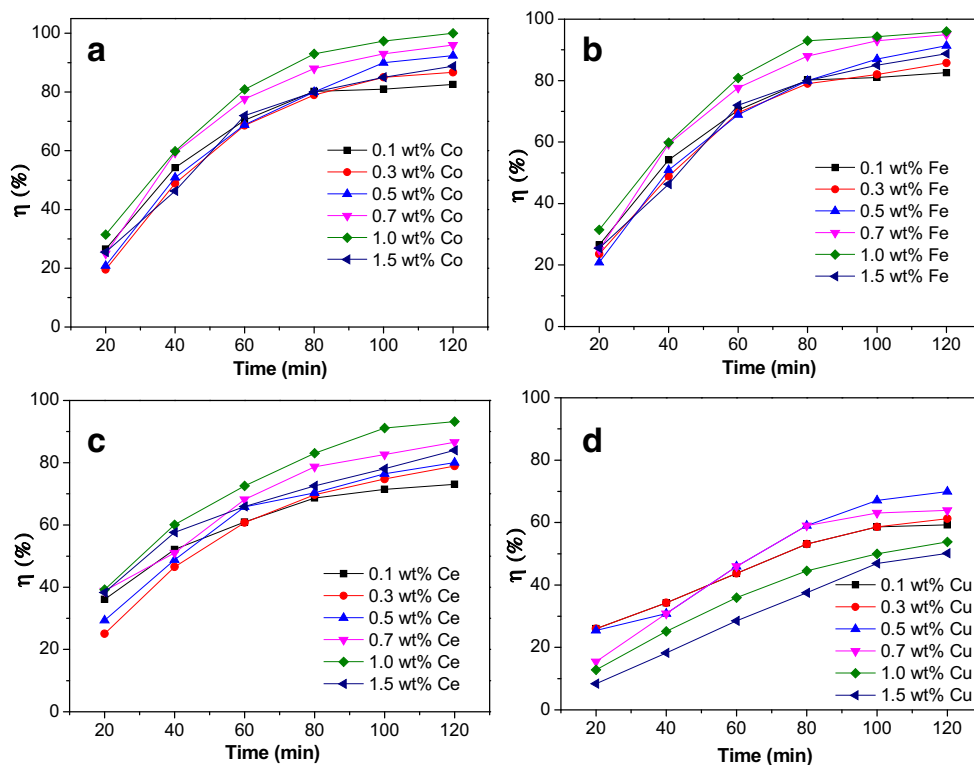
where  $n$  is the number of electrons transferred for oxygen reduction for  $H_2O_2$ ,  $F$  is the Faraday constant (96,485 C/mol),  $C$  is the concentration of  $H_2O_2$  (mol/L),  $V$  is the bulk volume (L),  $I$  is the current (A), and  $t$  is the electrolysis time (s).

The absorbance ( $A$ ) of MO was determined by the same spectrophotometer at a wavelength of 464 nm. The MO removal efficiency ( $\eta$ ) was calculated using the following formula:

$$\eta (\%) = \frac{A_0 - A_t}{A_0} \times 100 \quad (5)$$

where  $A_0$  and  $A_t$  denote the absorbance of the MO solution at initial and given time, respectively.

**Fig. 1** Effect of metal loadings on the degradation of MO: **a** Co, **b** Fe, **c** Ce, and **d** Cu. Conditions, 0.05 M  $Na_2SO_4$  and 50 mg/L MO; current density, 50 A/m<sup>2</sup> (pH = 3); air flow rate, 0.5 L/min



The total organic carbon (TOC) of the final sample in the EF process was determined by a TOC analyzer (Analytikjena multi N/C 3100, Germany).

Energy-related parameters are essential figures of merit for comparing the viability of EF and related methods between them and against other electro-chemical technologies. Operating at constant  $I$ , energy consumption per unit volume is obtained from the formula (6) (Brillas et al. 2009):

$$\text{Energy consumption (kWh m}^{-3}\text{)} = \frac{Ult}{V} \quad (6)$$

Where  $U$  is the average cell voltage (V),  $I$  is the current (A),  $t$  is the electrolysis time (h), and  $V$  is the bulk volume (L).

## Results and discussion

### Optimization of transition metal-based catalysts

In order to obtain the optimal mass ratio of the transition metal to carbon black for GF-metal, the performance of MO degradation was tested. As shown in Fig. 1, while metal content was low, with the increasing of mass ratio of the transition metal to carbon black, MO degradation improved, and then it decreased. The degradation efficiency reached the corresponding maximum of 99.2, 94.2, 89.5 and 70.1 % with 1 wt.% Co, 1 wt.% Fe, 1 wt.% Ce, and

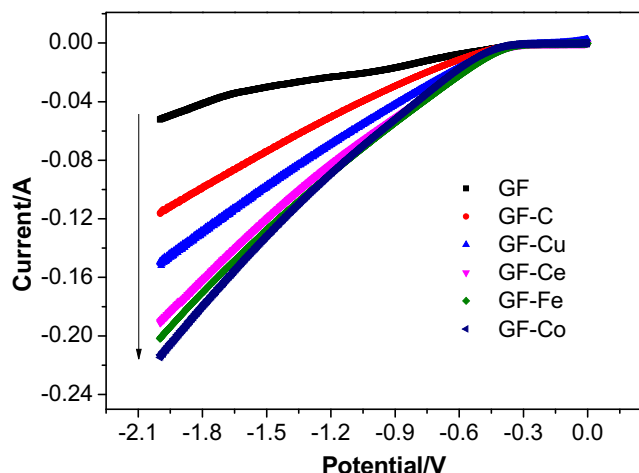


**Fig. 2** Linear sweep voltammograms. Conditions: scanning rate, 50 mV/s (0.05 M Na<sub>2</sub>SO<sub>4</sub>, pH 7), oxygen saturation

with excess transition metal ion, take Fe<sup>2+</sup> for example (Eq. 7) (Nidheesh and Gandhimathi 2012):



So 1 wt.% Co, 1 wt.% Fe, 1 wt.% Ce, and 0.5 wt.% Cu was selected as the best dosage for MO degradation, respectively.

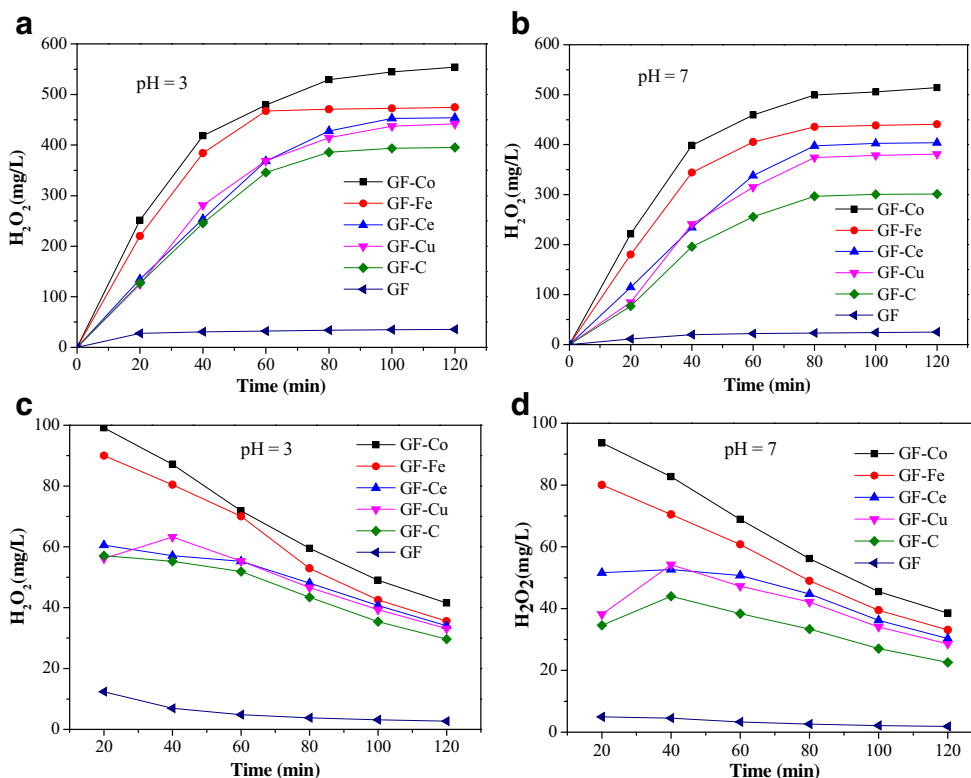
In order to investigate electro-catalytic activity of the as-prepared electrodes, LSV was carried out. As shown in Fig. 2, all transition metal-based electrodes exhibited higher current response for O<sub>2</sub> reduction than the GF without loading transition metal. This result indicated that the presence of transition metal was helpful for increasing the cathode conductivity and thus reducing the cathode potential. Among the transition metal-based electrodes, the GF-Co electrode showed the highest current response while the current response of GF-Cu electrode was the lowest. This trend was in agreement with that of MO removal, which is reasonable since the electro-chemical reaction rate is determined mainly by current (Yu et al. 2015b).

0.5 wt.% Cu, but for GF-C and GF the degradation efficiency were only 35.5 and 12.6 % within 120 min. It indicated that the MO removal efficiency significantly increased after transition metals were loaded. This was mainly due to more ·OH production with the existence of transition metal ions in the solution (Ai et al. 2013). However, a further increase of the transition metals content might cause an inhibition for MO degradation due to the loss of ·OH by reaction

### H<sub>2</sub>O<sub>2</sub> accumulation in the heterogeneous EF system

Since H<sub>2</sub>O<sub>2</sub> production is very important for electro-Fenton process, it is necessary to identify the H<sub>2</sub>O<sub>2</sub> production capacity of these transition metal-based cathodes. Figure 3a, b shows the

**Fig. 3** Effect of metal loading on (a, b) H<sub>2</sub>O<sub>2</sub> production and (c, d) current efficiency. Conditions, 0.05 M Na<sub>2</sub>SO<sub>4</sub>; current density, 50 A/m<sup>2</sup>; air flow rate, 0.5 L/min (1.0 wt.% Co, 1.0 wt.% Fe, 1.0 wt.% Ce, 0.5 wt.% Cu)



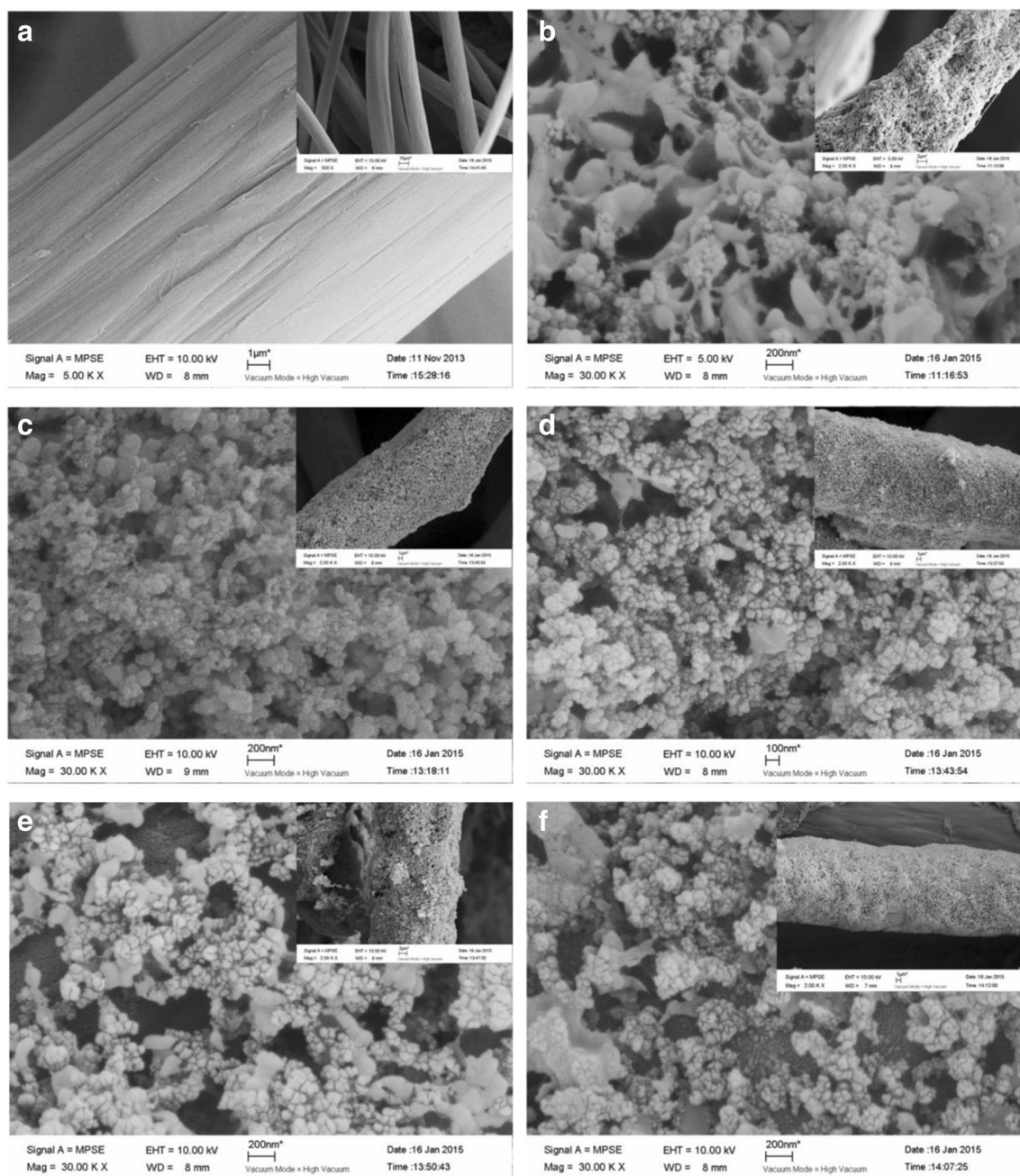


**Fig. 4** SEM image of **a** GF, **b** GF-C, **c** GF-Co, **d** GF-Fe, **e** GF-Ce, and **f** GF-Cu

accumulation of  $\text{H}_2\text{O}_2$  with different metal loadings at pH of 3 and 7, respectively. After 120 min electrolysis, the concentration of  $\text{H}_2\text{O}_2$  reached 554.8, 474.7, 454.1, 440, 380.5, and 35.6 mg/L at pH = 3 using GF-Co, GF-Fe, GF-Ce, GF-Cu, GF-C, and GF, respectively. Accordingly, the concentration of  $\text{H}_2\text{O}_2$  reached 516.8, 442.7, 404.1, 378.6, 315.2, and 25.5 mg/L at pH = 7. Similarly, GF-Co had the highest current efficiency for  $\text{H}_2\text{O}_2$  production (Fig. 3c, d), which reached 41 and 38 % in 2 h at pH 3 and 7, respectively. These results were in agreement with the LSV results (Fig. 2). The results indicated GF-Co had the highest catalytic activity for electro-reduction of  $\text{O}_2$  to

$\text{H}_2\text{O}_2$ . This was in agreement with other literatures (Bonakdarpour et al. 2011). There was a slight increase of the  $\text{H}_2\text{O}_2$  accumulation at pH 3 because a low pH was favorable to  $\text{H}_2\text{O}_2$  production (Eq. 1). In summary, the prepared GF-metal is a very good cathode material for  $\text{H}_2\text{O}_2$  production and potential to be used in electro-Fenton process.

#### Characterizations of the prepared electrodes

Figure 4 shows the SEM images of unmodified GF and modified GF. Before the transition metal was loaded,

the GF showed a clean fiber structure composed of an entangled network of carbon microfilaments with diameters around 15 μm. After the transition metal was loaded, a large numbers of interconnected particles appeared on the fiber of GF, which would obviously change the cathode surface characteristics. These carbon particles and porous structure on the electrode surface could promote O<sub>2</sub> electro-sorption and electro-reduction and pollutants degradation (Jin et al. 2011; Wu et al. 2010). Figure 4c shows GF-Co had a more uniform surface with particles, which might render GF-Co having the highest catalytic activity.

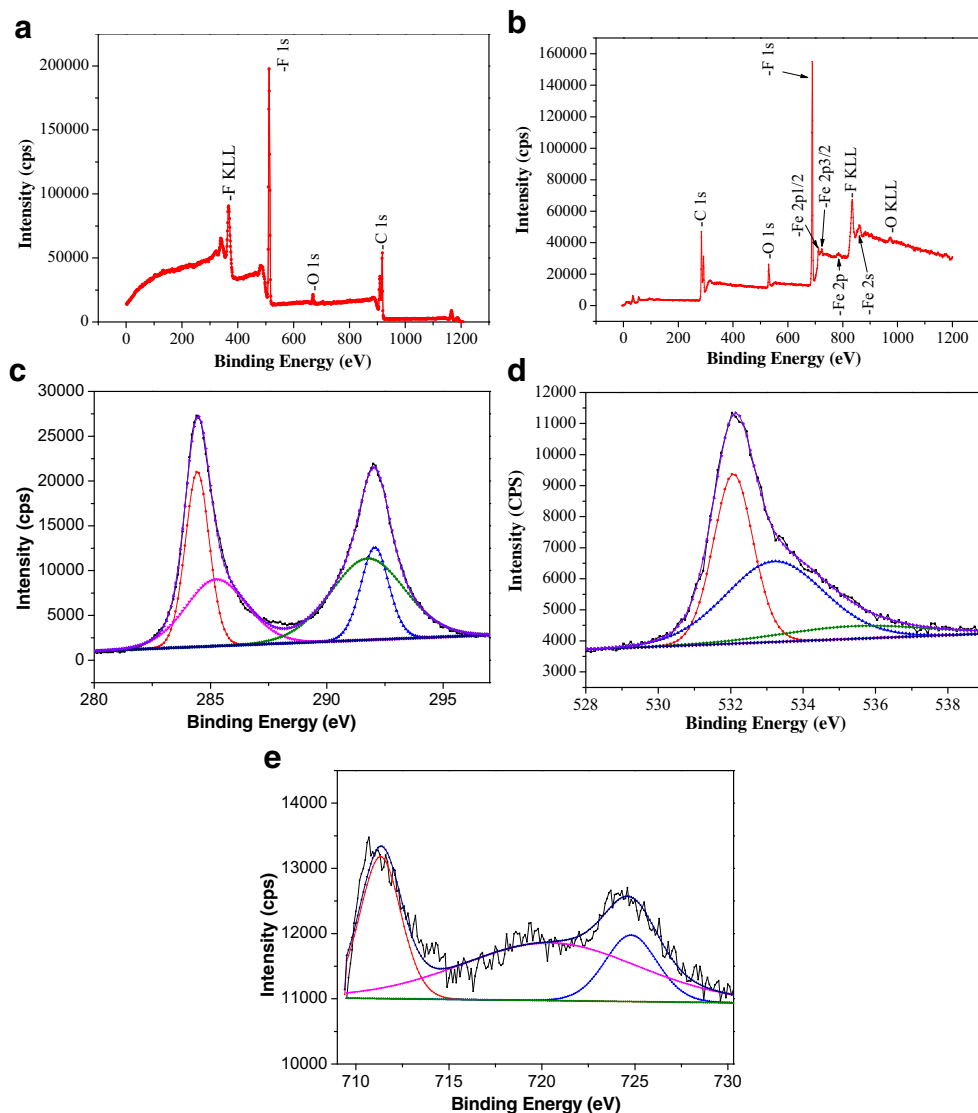
The surface element of the modified GF was studied by XPS analysis. Compared with GF-C (Fig. 5a), not only C and O elements but also iron element was observed and the ratio between O and C (O/C) increased in GF-Fe (Fig. 5b), which indicated that the number of

oxygen-containing functional groups increased after Fe was loaded. The F element was also detected, which was probably due to the addition of PTFE during modification.

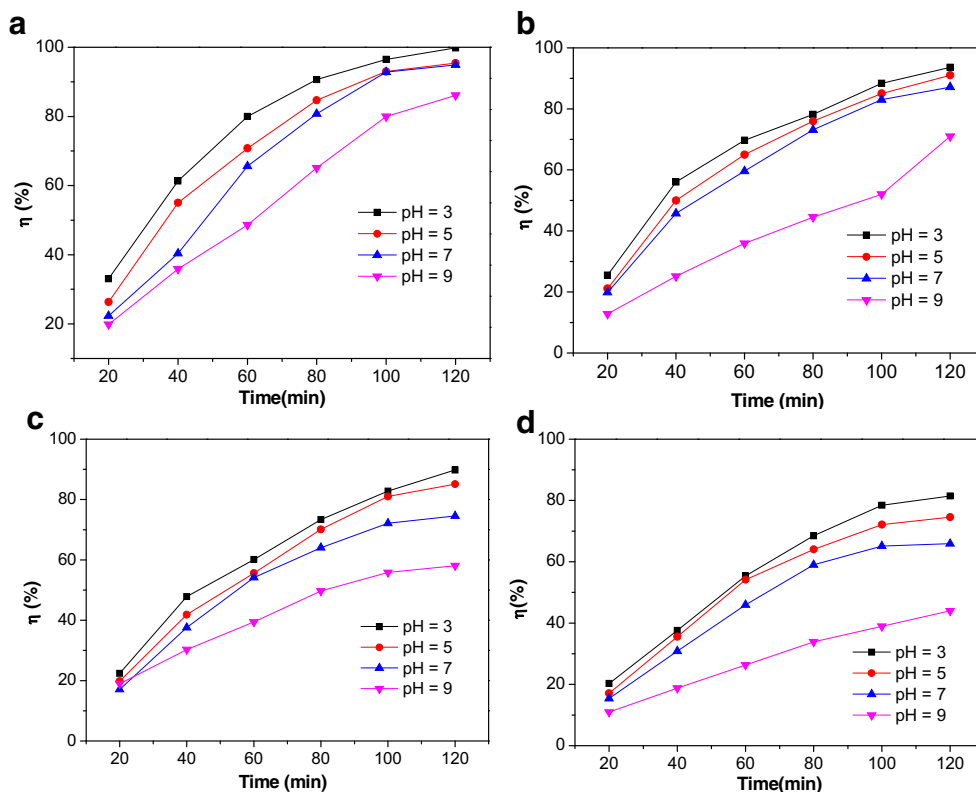
For GF-Fe, peak fitting of C1s and O1s were carried out, and the results are shown in Fig. 5c, d. Based on the literatures (Wang et al. 2013a), for C1s spectra, the main peak at 284.6–284.7 eV was attributed to graphitized carbon (C=C). The other three peaks should be attributed to the defects on the GF structure (C=C, 285.1 eV), C–OH (286.0–286.3 eV), and C–O (286.8–287.0 eV). Regarding the O1s spectra, the split peaks were located at 532.2–532.7, 531.0–531.1, and 533.9–534.2 eV, which should be assigned to O–H and C–O (Wang et al. 2015a).

Figure 5e presents the high-resolution spectra of Fe 2p. The peaks centered at 713.7 and 725.1 eV were assigned to Fe(III). The peak centered at 722.0 eV was attributed to

**Fig. 5** XPS of **a** GF-C and **b** GF-Fe; the high-resolution XPS spectrum of **c** C1s region, **d** O1s region, and **e** Fe2p region for GF-Fe



**Fig. 6** Effect of pH on the degradation of MO: **a** GF-Co, **b** GF-Fe, **c** GF-Ce, and **d** GF-Cu. Conditions, 0.05 M Na<sub>2</sub>SO<sub>4</sub> (50 mg/L MO); current density, 50 A/m<sup>2</sup>; air flow rate, 0.5 L/min (1.0 wt.% Co, 1.0 wt.% Fe, 1.0 wt.% Ce, 0.5 wt.% Cu)



Fe<sup>0</sup> (Ai et al. 2007a). Therefore, the iron species was mainly composed of Fe<sup>0</sup> and Fe<sub>2</sub>O<sub>3</sub>. These oxygen-containing groups and ferrite-carbon black hybrid could be acted as the active sites capable of accelerating the electro-chemical reactions and make dissolved oxygen accessible to the cathode surface facilitating electro-generation of H<sub>2</sub>O<sub>2</sub> (Miao et al. 2014).

### The degradation of MO in the heterogeneous EF system

It is well known that pH can remarkably affect Fenton reaction (Fan et al. 2010). In acid condition, soluble Fe<sup>2+</sup> can react with H<sub>2</sub>O<sub>2</sub> to produce ·OH which could degrade organic pollutants even into CO<sub>2</sub> and H<sub>2</sub>O, but in alkali condition, ferric species would precipitate as

ferric hydroxides, which made it more difficult to establish a good redox system between H<sub>2</sub>O<sub>2</sub> and Fe<sup>2+</sup>/Fe<sup>3+</sup> (Brillas et al. 2009). The degradation efficiency of MO with the optimum metal loading under different pH values is shown in Fig. 6. In general, degradation efficiency of MO decreased with an increase of pH, which accords with EF reaction. However, degradation efficiency of MO with 1.0 wt.% Co loading were 82 % within 120 min treatment even at pH 9 while 99 % at pH 3 (Fig. 6a), which was better than the results reported in other literatures (Torres

**Table 1** Final pH of the treated solution after 120 min

Initial pH	3	5	7	9
Final pH				
Co	3.2	3.6	3.7	3.6
Fe	3.0	4.7	5.4	7.7
Ce	3.1	4.7	5.4	6.5
Cu	3.1	4.5	5.0	8.5

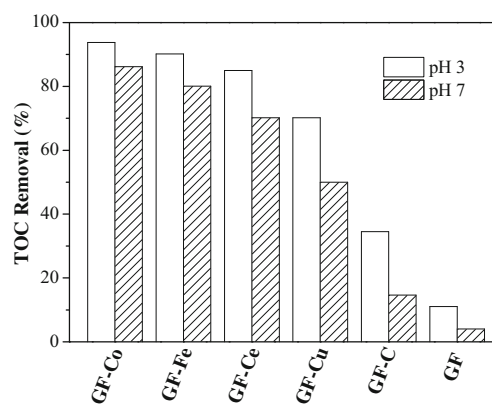


**Fig. 7** TOC removal using different cathodes at pH of 3 and 7 within 120 min treatment. Conditions, 0.05 M Na<sub>2</sub>SO<sub>4</sub> (50 mg/L MO); current density, 50 A/m<sup>2</sup>; air flow rate, 0.5 L/min (1.0 wt.% Co, 1.0 wt.% Fe, 1.0 wt.% Ce, 0.5 wt.% Cu)

**Table 2** The degradation kinetic rate constant (*k*) with different metal loading under different pH within 120 min treatment

<i>k</i> (s <sup>-1</sup> )	pH = 3	pH = 5	pH = 7	pH = 9
GF-Co	0.030	0.024	0.022	0.015
GF-Fe	0.021	0.020	0.016	0.0088
GF-Ce	0.017	0.015	0.013	0.0071
GF-Cu	0.014	0.012	0.010	0.006
GF-C	0.0065	0.005	0.004	0.0004
GF	0.0025	0.0018	0.0011	0.0001

et al. 2007; Zhang et al. 2015). According to the pH values in Table 1, the pH of solution at initial pH 3 remained almost unchanged during treatment while the solutions at pH ≥5 were strongly acidified, which was attributed to the formation of carboxylic acids (El-Ghenymy et al. 2012; Isarain-Chavez et al. 2010). This could explain why degradation efficiency of MO was still high even at alkali condition.

On the other hand, the kind of metal loading could affect the catalytic activity of the electrodes (Ai et al., 2007a, b, 2008). At pH 3, degradation efficiency of MO were 99, 93, 89, and 81 % with 1.0 wt.% Co, 1.0 wt.% Fe, 1.0 wt.% Ce, and 0.5 wt.% Cu, respectively. It indicated that GF-Co had the highest catalytic activity for H<sub>2</sub>O<sub>2</sub> electro-generation by O<sub>2</sub> electro-reduction and further heterogeneous EF process (Bonakdarpour et al. 2011). This result was also demonstrated in Fig. 7, in which the TOC removal efficiency was investigated with different metal loadings. At the pH of 3 and 7, the TOC removal efficiency were 93.8 and 86.2 %, 90.2 and 80.3 %, 85.1 and 70.2 %, 70 and 50.8 %, 35.2 and 14.4 %, and 12.3 and 4.5 % using GF-Co, GF-Fe, GF-Ce, GF-Cu, GF-C and GF, respectively. It proved that the electrodes had a better catalytic activity after loading metals. Compared with the degradation efficiency of MO, it also indicated that most of MO was mineralized into H<sub>2</sub>O and CO<sub>2</sub>. Table 2 shows that the degradation kinetic rate constant (*k*) with different metal loadings under different pH values, which was obtained by assuming a pseudo-first reaction rate and could explain the degradation trends more directly. The degradation kinetic rate constant

decreased with an increase of pH and also as following order at the same pH: GF-Co, GF-Fe, GF-Ce, GF-Cu, GF-C, and GF. Particularly, when using GF at pH 3, the degradation kinetic rate constant was 0.0025 s<sup>-1</sup>, which was 25 times higher than that at pH 9, but the degradation kinetic rate constant was 0.030 s<sup>-1</sup> using GF-Co at pH 3, which was two times higher than that at pH 9. This result demonstrated again that GF-Co had the high catalytic activity for MO degradation at a wide pH range.

**Stability test and performance comparison**

Since the stability of an electrode is important for practical application, the performance of GF-Co in ten-time

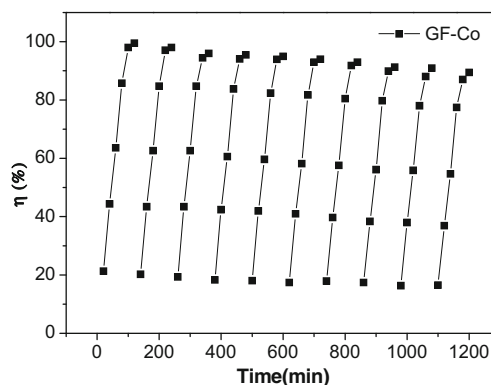


**Fig. 8** The stability test of GF-Co in ten-time continuous runs. Conditions, 0.05 M Na<sub>2</sub>SO<sub>4</sub> (50 mg/L MO); current density, 50 A/m<sup>2</sup> (pH = 3, 1.0 wt.% Co)



**Table 3** Comparison of MO degradation with other literatures

	$C_0$ (mg L <sup>-1</sup> )	$j$ (mA cm <sup>-2</sup> )	Time (h)	Degradation efficiency (%)	TOC removal (%)	Energy consumption	Reference
PbO <sub>2</sub> anode	0.25 mM	0.6 A	2	100	28		Recio et al. (2011)
Three-dimensional electrodes	1150	2 A	0.67		94 (COD)	14.6 kWh (kg COD) <sup>-1</sup>	Liu et al. (2011)
Ti/BDD anode	100	31	2.3	96	60 (COD)	7.7 kWh m <sup>-3</sup>	Ramírez et al., (2013)
E-Fenton	100	500 mA	1	72			Isarain-Chavez et al. (2013)
Photo- E-Fenton	500	135 mA	1.5	100	71		Zhao et al. (2010)
E-Fenton-like	50	5	2	99	93	7.0 kWh m <sup>-3</sup>	Present work

continuous runs was investigated for MO degradation. As shown in Fig. 8, the MO degradation efficiency was almost stable with a slight decrease during the ten-time runs. At the first time, the MO degradation efficiency was 99.5 % at pH 3 within 120 min treatment and at the tenth time, that was still 89.5 %. It indicated that the GF-Co electrode was relatively stable and reusable during the process of MO removal. The obtained results demonstrated that the GF-Co electrode had good stability, which was promising for long-term practical application.

Table 3 shows the comparison of the results of MO degradation with other literatures. In the present work, the energy consumption for MO degradation within 2 h was only 7.0 kWh m<sup>-3</sup>, which was lower than the result of the experiment using Ti/BDD anode (Ramírez et al. 2013). And the TOC removal efficiency using GDE/Co as heterogeneous EF like was 93 %, which was higher than the result using PbO<sub>2</sub> anode (Recio et al. 2011). These results indicated that the heterogeneous EF like using GDE/Co shows a high degradation efficiency and

TOC removal for and a low-energy consumption MO degradation.

### Confirmation of hydroxyl radical

Hydroxyl radical oxidation is a key mechanism in AOPs. To identify the function of  $\cdot\text{OH}$ , a hydroxyl radical scavenger, isopropanol (Richard et al. 1997), was added to the solution during degradation of MO. The effect of isopropanol (IPA) addition on the degradation efficiency of MO is shown in Fig. 9. Without IPA, the degradation efficiency of MO was 99 and 94 % at pH 3 and 7 within 120 min treatment. However, after IPA was added into the solution, the degradation efficiency of MO decreased to 21 and 27 %, respectively. This result indicated that the addition of isopropanol obviously inhibited the degradation efficiency of MO and  $\cdot\text{OH}$  played an important role in MO degradation.

### Conclusions

In this work, feasibility of GF-metal was demonstrated in the heterogeneous EF process for MO degradation. After loading metals, the value of O/C increased observed by XPS, the current response became higher and the degradation efficiency of MO was improved. In the H<sub>2</sub>O<sub>2</sub> production experiment, GF-Co was proved to have the highest catalytic activity for electro-reduction of O<sub>2</sub> to H<sub>2</sub>O<sub>2</sub>. With an increase of pH, the degradation efficiency of MO decreased slightly, but even at initial pH 9, 82 % of MO degradation efficiency was obtained using GF-Co after 120 min treatment. In the process of MO degradation at initial pH  $\geq 5$ , pH of solution decreased. TOC results indicated that most of MO was mineralized into H<sub>2</sub>O and CO<sub>2</sub>. GF-Co had a high stability for MO degradation even after ten-time runs. The addition of isopropanol proved that  $\cdot\text{OH}$  played an important role in degradation of MO. The results show the GF-Co is very promising for wastewater treatment.

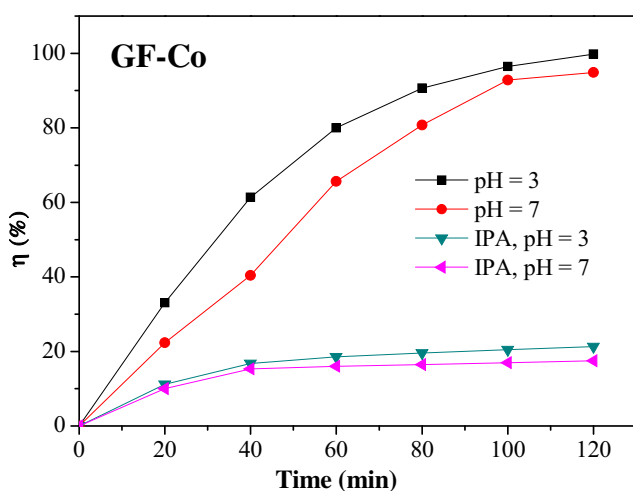


**Fig. 9** Effect of isopropanol on degradation of MO using GF-Co. Conditions, 0.05 M Na<sub>2</sub>SO<sub>4</sub> (50 mg/L MO); current density, 50 A/m<sup>2</sup> (1.0 wt.% Co, 5 mL IPA)

**Acknowledgments** This work was supported by Natural Science Foundation of China (no. 21273120 and 51178225), National High Technology Research and Development Program of China (2013AA065901 and 2013AA06A205), and National Special S&T Project on Water Pollution Control and Management (2015ZX07203-011).

## References

- Ai ZH, Gao ZT, Zhang LZ, He WW, Yin JJ (2013) Core-shell structure dependent reactivity of Fe@Fe<sub>2</sub>O<sub>3</sub> nanowires on aerobic degradation of 4-chlorophenol. *Environ Sci Technol* 47:5344–5352. doi:10.1021/es4005202
- Ai ZH, Lu LR, Li JP, Zhang LZ, Qiu JR, Wu MH (2007a) Fe@Fe<sub>2</sub>O<sub>3</sub> core-shell nanowires as the iron reagent. 2. An efficient and reusable sono-Fenton system working at neutral pH. *J Phys Chem C* 111:7430–7436. doi:10.1021/jp070412v
- Ai ZH, Mei T, Liu J, Li JP, Jia FL, Zhang LZ, Qiu JR (2007b) Fe@Fe<sub>2</sub>O<sub>3</sub> core-shell nanowires as an iron reagent. 3. Their combination with CNTs as an effective oxygen-fed gas diffusion electrode in a neutral electro-Fenton system. *J Phys Chem C* 111:14799–14803. doi:10.1021/jp073617c
- Ai ZH, Xiao HY, Mei T, Liu J, Zhang LZ, Deng KJ, Qiu JR (2008) Electro-Fenton degradation of rhodamine B based on a composite cathode of Cu<sub>2</sub>O nanocubes and carbon nanotubes. *J Phys Chem C* 112:11929–11935. doi:10.1021/jp803243t
- Ammar S, Oturan MA, Labiadh L, Guersalli A, Abdelhedi R, Oturan N, Brillas E (2015) Degradation of tyrosol by a novel electro-Fenton process using pyrite as heterogeneous source of iron catalyst. *Water Res* 74:77–87. doi:10.1016/j.watres.2015.02.006
- Bonakdarpour A, Esau D, Cheng H, Wang A, Gyenge E, Wilkinson DP (2011) Preparation and electrochemical studies of metal-carbon composite catalysts for small-scale electrosynthesis of H<sub>2</sub>O<sub>2</sub>. *Electrochim Acta* 56:9074–9081. doi:10.1016/j.electacta.2011.06.043
- Brillas E, Calpe JC, Casado J (2000) Mineralization of 2,4-D by advanced electrochemical oxidation processes. *Water Res* 34:2253–2262. doi:10.1016/S0043-1354(99)00396-6
- Brillas E, Martinez-Huitle CA (2015) Decontamination of wastewaters containing synthetic organic dyes by electrochemical methods. An updated review. *Appl Catal B-Environ* 166:603–643. doi:10.1016/j.apcatb.2014.11.016
- Brillas E, Sirés I, Oturan MA (2009) Electro-Fenton process and related electrochemical technologies based on Fenton's reaction chemistry. *Chem Rev* 109:6570–6631. doi:10.1021/cr900136g
- Dhakshinamoorthy A, Navalon S, Alvaro M, Garcia H (2012) Metal nanoparticles as heterogeneous Fenton catalysts. *ChemSusChem* 5:46–64. doi:10.1002/cssc.201100517
- El-Ghenymy A, Garrido JA, Centellas F, Arias C, Cabot PL, Rodriguez RM, Brillas E (2012) Electro-Fenton and photoelectro-Fenton degradation of sulfanilic acid using a boron-doped diamond anode and an air diffusion cathode. *J Phys Chem A* 116:3404–3412. doi:10.1021/jp300442y
- Fan Y, Ai ZH, Zhang LZ (2010) Design of an electro-Fenton system with a novel sandwich film cathode for wastewater treatment. *J Hazard Mater* 176:678–684. doi:10.1016/j.jhazmat.2009.11.085
- Feng HM, Zheng JC, Lei NY, Yu L, Kong KHK, Yu HQ, Lau TC, Lam MHW (2011) Photoassisted Fenton degradation of polystyrene. *Environ Sci Technol* 45:744–750. doi:10.1021/es102182g
- García-Segura S, Garrido JA, Rodríguez RM, Cabot PL, Centellas F, Arias C, Brillas E (2012) Mineralization of flumequine in acidic medium by electro-Fenton and photoelectro-Fenton processes. *Water Res* 46:2067–2076. doi:10.1016/j.watres.2012.01.019
- Huang RX, Fang ZQ, Yan XM, Cheng W (2012) Heterogeneous sono-Fenton catalytic degradation of bisphenol A by Fe<sub>3</sub>O<sub>4</sub> magnetic nanoparticles under neutral condition. *Chem Eng J* 197:242–249. doi:10.1016/j.cej.2012.05.035
- Isarain-Chavez E, Arias C, Cabot PL, Centellas F, Rodriguez RM, Garrido JA, Brillas E (2010) Mineralization of the drug beta-blocker atenolol by electro-Fenton and photoelectro-Fenton using an air-diffusion cathode for H<sub>2</sub>O<sub>2</sub> electrogeneration combined with a carbon-felt cathode for Fe<sup>2+</sup> regeneration. *Appl Catal B-Environ* 96:361–369. doi:10.1016/j.apcatb.2010.02.033
- Isarain-Chavez E, de la Rosa C, Martinez-Huitle CA, Peralta-Hernandez JM (2013) On-site hydrogen peroxide production at pilot flow plant: application to electro-Fenton process. *Int J Electrochem Sci* 8:3084–3094
- Jin YN, Zhao GH, Wu MF, Lei YZ, Li MF, Jin XP (2011) In situ induced visible-light photoelectrocatalytic activity from molecular oxygen on carbon aerogel-supported TiO<sub>2</sub>. *J Phys Chem C* 115:9917–9925. doi:10.1021/jp2009429
- Liang XL, Zhong YH, Zhu SY, Ma LY, Yuan P, Zhu JX, He HP, Jiang Z (2012) The contribution of vanadium and titanium on improving methylene blue decolorization through heterogeneous UV-Fenton reaction catalyzed by their co-doped magnetite. *J Hazard Mater* 199:247–254. doi:10.1016/j.jhazmat.2011.11.007
- Liu Z, Wang F, Li Y, Xu T, Zhu S (2011) Continuous electrochemical oxidation of methyl orange waste water using a three-dimensional electrode reactor. *J Environ Sci* 23:S70–S73. doi:10.1016/s1001-0742(11)61081-4
- Martinez-Huitle CA, Rodrigo MA, Sirés I, Sialdone O (2015) Single and coupled electrochemical processes and reactors for the abatement of organic water pollutants: a critical review. *Chem Rev* 115:13362–13407. doi:10.1021/acs.chemrev.5b00361
- Miao J, Zhu H, Tang Y, Chen YM, Wan PY (2014) Graphite felt electrochemically modified in H<sub>2</sub>SO<sub>4</sub> solution used as a cathode to produce H<sub>2</sub>O<sub>2</sub> for pre-oxidation of drinking water. *Chem Eng J* 250:312–318. doi:10.1016/j.cej.2014.03.043
- Navalon S, Dhakshinamoorthy A, Alvaro M, Garcia H (2011) Heterogeneous Fenton catalysts based on activated carbon and related materials. *ChemSusChem* 4:1712–1730. doi:10.1002/cssc.201100216
- Nidheesh PV, Gandhimathi R (2012) Trends in electro-Fenton process for water and wastewater treatment: an overview. *Desalination* 299:1–15. doi:10.1016/j.desal.2012.05.011
- Oturan N, Wu J, Zhang H, Sharma VK, Oturan MA (2013) Electrocatalytic destruction of the antibiotic tetracycline in aqueous medium by electrochemical advanced oxidation processes: effect of electrode materials. *Appl Catal B-Environ* 140:92–97. doi:10.1016/j.apcatb.2013.03.035
- Özcan A, Sahin Y, Koparal AS, Oturan MA (2008) Carbon sponge as a new cathode material for the electro-Fenton process: comparison with carbon felt cathode and application to degradation of synthetic dye basic blue 3 in aqueous medium. *J Electroanal Chem* 616:71–78. doi:10.1016/j.jelechem.2008.01.002
- Özcan A, Sahin Y, Koparal AS, Oturan MA (2009) A comparative study on the efficiency of electro-Fenton process in the removal of prophan from water. *Appl Catal B-Environ* 89:620–626. doi:10.1016/j.apcatb.2009.01.022
- Panizza M, Oturan MA (2011) Degradation of alizarin red by electro-Fenton process using a graphite-felt cathode. *Electrochim Acta* 56:7084–7087. doi:10.1016/j.electacta.2011.05.105
- Pimentel M, Oturan N, Dezotti M, Oturan MA (2008) Phenol degradation by advanced electrochemical oxidation process electro-Fenton using a carbon felt cathode. *Appl Catal B-Environ* 83:140–149. doi:10.1016/j.apcatb.2008.02.011
- Ramírez C, Saldaña A, Hernández B, Acero R, Guerra R, García-Segura S, Brillas E, Peralta-Hernandez JM (2013) Electrochemical oxidation of methyl orange azo dye at pilot flow plant using BDD technology. *J Ind Eng Chem* 19:571–579. doi:10.1016/j.jiec.2012.09.010
- Recio FJ, Herrasti P, Sirés I, Kulak AN, Bavykin DV, Ponce-de-León C, Walsh FC (2011) The preparation of PbO<sub>2</sub> coatings on reticulated

- vitreous carbon for the electro-oxidation of organic pollutants. *Electrochim Acta* 56:5158–5165. doi:10.1016/j.electacta.2011.03.054
- Richard C, Bosquet F, Pilichowski JF (1997) Photocatalytic transformation of aromatic compounds in aqueous zinc oxide suspensions: effect of substrate concentration on the distribution of products. *J Photoch Photobio A-Chem* 108:45–49. doi:10.1016/S1010-6030(96)04431-0
- Scialdone O, Galia A, Sabatino S (2013) Electro-generation of H<sub>2</sub>O<sub>2</sub> and abatement of organic pollutant in water by an electro-Fenton process in a microfluidic reactor. *Electrochem Commun* 26:45–47. doi:10.1016/j.elecom.2012.10.006
- Segura Y, Martinez F, Melero JA, Molina R, Chand R, Bremner DH (2012) Enhancement of the advanced Fenton process (Fe<sup>0</sup>/H<sub>2</sub>O<sub>2</sub>) by ultrasound for the mineralization of phenol. *Appl Catal B-Environ* 113:100–106. doi:10.1016/j.apcatb.2011.11.024
- Sirés I, Brillas E, Oturan MA, Rodrigo MA, Panizza M (2014) Electrochemical advanced oxidation processes: today and tomorrow. A review. *Environ Sci Pollut R* 21:8336–8367. doi:10.1007/s11356-014-2783-1
- Torres RA, Abdelmalek F, Combet E, Petrier C, Pulgarin C (2007) A comparative study of ultrasonic cavitation and Fenton's reagent for bisphenol a degradation in deionised and natural waters. *J Hazard Mater* 146:546–551. doi:10.1016/j.jhazmat.2007.04.056
- Valdes-Solis T, Valle-Vigón P, Alvarez S, Marban G, Fuertes AB (2007) Manganese ferrite nanoparticles synthesized through a nanocasting route as a highly active Fenton catalyst. *Catal Commun* 8:2037–2042. doi:10.1016/j.catcom.2007.03.030
- Wang AM, Qu JH, Ru J, Liu HJ, Ge JT (2005) Mineralization of an azo dye acid red 14 by electro-Fenton's reagent using an activated carbon fiber cathode. *Dyes Pigments* 65:227–233. doi:10.1016/j.dyepig.2004.07.019
- Wang Y, Liu YH, Wang K, Song SQ, Tsiakaras P, Liu H (2015a) Preparation and characterization of a novel KOH activated graphite felt cathode for the electro-Fenton process. *Appl Catal B-Environ* 165:360–368. doi:10.1016/j.apcatb.2014.09.074
- Wang YB, Zhao HY, Zhao GH (2015b) Iron-copper bimetallic nanoparticles embedded within ordered mesoporous carbon as effective and stable heterogeneous Fenton catalyst for the degradation of organic contaminants. *Appl Catal B-Environ* 164:396–406. doi:10.1016/j.apcatb.2014.09.047
- Wang YJ, Zhao GH, Chai SN, Zhao HY, Wang YB (2013a) Three-dimensional homogeneous ferrite-carbon aerogel: one pot fabrication and enhanced electro-Fenton reactivity. *ACS Appl Mater Inter* 5:842–852. doi:10.1021/am302437a
- Wang YJ, Zhao HY, Chai SN, Wang YB, Zhao GH, Li DM (2013b) Electrosorption enhanced electro-Fenton process for efficient mineralization of imidacloprid based on mixed-valence iron oxide composite cathode at neutral pH. *Chem Eng J* 223:524–535. doi:10.1016/j.cej.2013.03.016
- Wu MF, Jin YN, Zhao GH, Li MF, Li DM (2010) Electrosorption-promoted photodegradation of opaque wastewater on a novel TiO<sub>2</sub>/carbon aerogel electrode. *Environ Sci Technol* 44:1780–1785. doi:10.1021/es903201m
- Yu FK, Zhou MH, Yu XM (2015a) Cost-effective electro-Fenton using modified graphite felt that dramatically enhanced on H<sub>2</sub>O<sub>2</sub> electro-generation without external aeration. *Electrochim Acta* 163:182–189. doi:10.1016/j.electacta.2015.02.166
- Yu XM, Zhou MH, Ren GB, Ma L (2015b) A novel dual gas diffusion electrodes system for efficient hydrogen peroxide generation used in electro-Fenton. *Chem Eng J* 263:92–100. doi:10.1016/j.cej.2014.11.053
- Zhang C, Zhou MH, Ren GB, Yu XM, Ma L, Yang J, Yu FK (2015) Heterogeneous electro-Fenton using modified iron-carbon as catalyst for 2,4-dichlorophenol degradation: influence factors, mechanism and degradation pathway. *Water Res* 70:414–424. doi:10.1016/j.watres.2014.12.022
- Zhang GQ, Wang S, Yang FL (2012) Efficient adsorption and combined heterogeneous/homogeneous Fenton oxidation of amaranth using supported nano-FeOOH as cathodic catalysts. *J Phys Chem C* 116:3623–3634. doi:10.1021/jp210167b
- Zhang GQ, Yang FL, Gao MM, Fang XH, Liu LF (2008a) Electro-Fenton degradation of azo dye using polypyrrole/anthraquinonedisulphonate composite film modified graphite cathode in acidic aqueous solutions. *Electrochim Acta* 53:5155–5161. doi:10.1016/j.electacta.2008.01.008
- Zhang GQ, Yang FL, Gao MM, Liu LF (2008b) Electrocatalytic behavior of the bare and the anthraquinonedisulfonate/polypyrrole composite film modified graphite cathodes in the electro-Fenton system. *J Phys Chem C* 112:8957–8962. doi:10.1021/jp800757v
- Zhang XW, Fu JL, Zhang Y, Lei LC (2008c) A nitrogen functionalized carbon nanotube cathode for highly efficient electrocatalytic generation of H<sub>2</sub>O<sub>2</sub> in electro-Fenton system. *Sep Purif Technol* 64:116–123. doi:10.1016/j.seppur.2008.07.020
- Zhang XW, Lei LC, Xia B, Zhang Y, Fu JL (2009) Oxidization of carbon nanotubes through hydroxyl radical induced by pulsed O<sub>2</sub> plasma and its application for O<sub>2</sub> reduction in electro-Fenton. *Electrochim Acta* 54:2810–2817. doi:10.1016/j.electacta.2008.11.029
- Zhao HY, Wang YJ, Wang YB, Cao TC, Zhao GH (2012) Electro-Fenton oxidation of pesticides with a novel Fe<sub>3</sub>O<sub>4</sub>@Fe<sub>2</sub>O<sub>3</sub>/activated carbon aerogel cathode: high activity, wide pH range and catalytic mechanism. *Appl Catal B-Environ* 125:120–127. doi:10.1016/j.apcatb.2012.05.044
- Zhao KJ, Zhao GH, Li PQ, Gao JX, Lv BY, Li DM (2010) A novel method for photodegradation of high-chroma dye wastewater via electrochemical pre-oxidation. *Chemosphere* 80:410–415. doi:10.1016/j.chemosphere.2010.04.019
- Zhao YB, Pan F, Li H, Niu TC, Xu GQ, Chen W (2013) Facile synthesis of uniform alpha-Fe<sub>2</sub>O<sub>3</sub> crystals and their facet-dependent catalytic performance in the photo-Fenton reaction. *J Mater Chem A* 1:7242–7246. doi:10.1039/c3ta10966f
- Zhou L, Zhou MH, Hu ZX, Bi ZH, Serrano KG (2014) Chemically modified graphite felt as an efficient cathode in electro-Fenton for p-nitrophenol degradation. *Electrochim Acta* 140:376–383. doi:10.1016/j.electacta.2014.04.090
- Zhou MH, Tan QQ, Wang Q, Jiao YL, Oturan N, Oturan MA (2012) Degradation of organics in reverse osmosis concentrate by electro-Fenton process. *J Hazard Mater* 215:287–293. doi:10.1016/j.jhazmat.2012.02.070